Available online at www.sciencedirect.com
SCIENCE DIRECT®
Journal of Catalysis 220 (2003) 273–279
JOURNAL OF CATALYSIS
www.elsevier.com/locate/jcat

Ammonia synthesis over a Ru(0001) surface studied by density functional calculations

Á. Logadóttir and J.K. Nørskov *

Center for Atomic-Scale Materials Physics, Department of Physics, Technical University of Denmark, DK-2800 Lyngby, Denmark

Received 8 January 2003; revised 17 March 2003; accepted 17 March 2003

Abstract

In this paper we present DFT studies of all the elementary steps in the synthesis of ammonia from gaseous hydrogen and nitrogen over a ruthenium crystal. The stability and configurations of intermediates in the ammonia synthesis over a Ru(0001) surface have been investigated, both over a flat surface and over a stepped surface. The calculations show that the step sites on the surface are much more reactive than the terrace sites. The DFT results are then used to study the mechanism of promotion by alkalies over the Ru(0001) and to determine the rate-determining step in the synthesis of ammonia over the Ru catalyst.

Keywords: Density functional calculations; Ruthenium; Ammonia; Reaction mechanism; Kinetics; Promotion

1. Introduction

In the Haber–Bosch process ammonia is synthesized directly from gaseous nitrogen and hydrogen over catalytic particles. The catalyst mostly used is based on iron [1], but ruthenium is more active and a ruthenium-based catalyst has been commercialized recently [2,3]. The catalyst is, however, not nearly as common as the iron catalyst due to the high price of ruthenium and the shorter lifetime of the catalyst [4].

In the following we will outline the detailed reaction mechanism for ammonia synthesis over Ru.

The first step in the reaction over a Ru surface, the N_2 dissociation, has been widely studied experimentally [5–10]. Other steps in the reaction have also been investigated in experiments [11–18]. This is usually done either by decomposition of NH_3 [15], N_2H_4 [16], or NH_2CHO [17] or by letting adsorbed nitrogen and hydrogen react [18]. The reaction intermediates can then be identified by their vibrational spectra, and in this way adsorption sites and configurations can be deduced for the surface species present [11,14,19,20]. The adsorption of the reaction intermediates, especially NH_3, is the subject of many discussions [14,17,18]. For the NH_3 molecule, thermal desorption spectroscopy (TDS) studies show two different chemisorption states, denoted α_1 and α_2 [14]. The α_1 state desorbs at about 310 K and is the only one present at low coverages. At higher coverages both states are seen with α_2 desorbing at about 180 K. The adsorption sites and geometries of these two states have not been found with certainty but both the on-top site and the hollow site, and even the coexistence of both of them, have been suggested [14,17,21].

Also theoretical studies have directed their attention to NH_3 synthesis over a Ru surface, but DFT studies for other steps in the reaction than the N_2 dissociation [22–26] are rather few. An estimate of the energetics along the reaction path was first presented by Rod et al. [27] and later by Zhang et al. [28], who in addition to adsorption also estimated the barriers for the hydrogenation steps in the reaction. Zhang et al. included the influence of step sites on the surface for parts of the process in their study, but they concluded that the effect is small.

Calculations have also been used as a tool in the identification of reaction intermediates on the surface. This has been done by calculating vibrational frequencies for an intermediate and comparing it to the frequencies found in the experiments discussed above [20,29,30]. The adsorption energies and vibrational frequencies have been estimated with DFT both for the NH_3 molecule [29] and the NH species [20]. The subject of the former calculations was the adsorption of

* Corresponding author.
E-mail address: norskov@fysik.dtu.dk (J.K. Nørskov).

0021-9517/$ – see front matter
doi:10.1016/S0021-9517(03)00156-8

NH_3 on a Ru cluster [29,30]. From these calculations and comparison with experiments they suggest a threefold hollow site as the most stable adsorption site for NH_3. From the DFT calculations for NH adsorbed on a Ru cluster Staufer et al. [20] suggest the same adsorption site for NH.

Below we present our results from DFT calculations for all the elementary steps in the reaction over a Ru(0001) surface. First we describe the calculational method. Then the adsorption of reaction intermediates will be considered in addition to the reaction barriers. The promotion mechanism over the Ru(0001) surface is next studied and finally we use the results from the DFT calculations to confirm that the rate-limiting step of the reaction over the Ru(0001) surface is the N_2 dissociation.

2. Methods

To calculate adsorption energies and reaction barriers for the synthesis of ammonia over Ru(0001) we use density functional (DFT) calculations. The DFT calculations are based on a plane-wave expansion of the wavefunctions, a RPBE description of exchange and correlation effects [31], and ultrasoft pseudopotentials [32]. Plane waves with kinetic energy up to 25 Ry are used. The self-consistent electron density is determined by iterative diagonalization of the Kohn–Sham Hamiltonian, Fermi-population of the Kohn–Sham states ($k_BT = 0.1$ eV), and Pulay mixing of the resulting electronic density [33]. All total energies have been extrapolated to $k_BT = 0$ eV.

Two model systems were used to describe the Ru(0001) surface, one for terraces on the crystal and another for the steps on the surface. In both cases the surface was modeled by a periodic array of slabs. In the model for the flat surface we used two-layer slabs and a (2×2) surface unit cell. The surface atoms are kept fixed at their bulk positions and the slabs are separated by 11 Å of vacuum. The effect of not relaxing the surface atoms has been tested. These calculations showed that by relaxing the top surface layer increased the adsorption energy of N on the surface by only 0.04 eV.

The choice of a two-layer slab for the terrace model can be justified by the test shown in Fig. 1a. The energy for the slabs with a different number of layers is determined, and it can be seen that its variation with the number of layers is quite small. Thus the minimum number of layers, namely two, is chosen in order to save computational time. The use of such a small unit cell will introduce some degree of error to the results but the accuracy was estimated to be sufficient for the comparison made here. Fig. 1b shows the atomic N adsorption energy for different sizes of surface unit cells. The adsorption energy is nearly the same for the (2×2) unit cell and the (3×2) unit cell. This indicates that interactions between the adsorbate are the same at these surface coverages of N. The smaller unit cell is therefore chosen in the calculations for the terrace site.

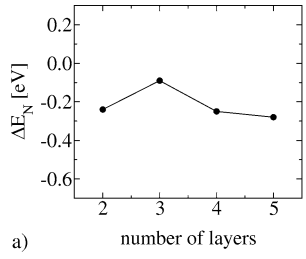

unit cell	θ	ΔE_N [eV]
(1×1)	0.50	0.12
(2×2)	0.25	-0.28
(3×2)	0.17	-0.29

Fig. 1. The adsorption energy (ΔE_N) of an atomic nitrogen on a Ru(0001) as a function of (a) number of layers and (b) surface coverage. The reference energy is the clean Ru slab and the N_2 molecule in the gas phase. The use of two layers introduces only about 0.05 eV error compared to the more converged results using four- and five-layer slabs.

The stepped surface is also modeled by two-layer slab with 11 Å of vacuum between the slabs. A step is made on the surface by adding two Ru rows on one side of the slab. In this case a (4×2) unit cell is used. In the stepped Ru surface the two top layers are allowed to relax.

To find the barriers for each step in the reaction, we use two different methods. For N_2 dissociation the initial and final state were first found. Then the bond length between the two N atoms was kept fixed and the system allowed to relax. This was repeated with a longer N–N bond length until the molecule had dissociated. By also keeping track of the forces between the N atoms it is possible to locate the transition state. The approach assumes that the N–N bond length is close to the reaction coordinates. This has been shown to be true for N_2 dissociation on Ru(0001) [22]. Not all reaction paths are as simple as the one for N_2 dissociation. For more complex reactions, where only the substrate and the product are known, we use the nudged elastic band method (NEB) to determine the reaction path [34,35].

3. Results and discussions

The reaction mechanism for the NH_3 synthesis on a Ru surface has not been completely established but is believed to be similar to the one on Fe surfaces. For the Fe catalyst, however, the detailed mechanism for NH_3 synthesis is known and the elementary steps in the reaction are [36,37]

$$N_2 + 2* \rightarrow 2N*, \tag{1}$$

$$H_2 + 2* \rightleftarrows 2H*, \tag{2}$$

$$N* + H* \rightleftarrows NH* + *, \tag{3}$$

$$NH* + H* \rightleftarrows NH_2* + *, \tag{4}$$

$$NH_2* + H* \rightleftarrows NH_3* + *, \tag{5}$$

$$NH_3* \rightleftarrows NH_3 + *, \tag{6}$$

where $*$ stands for an empty site on the surface. It has been shown that the first reaction is rate-determining and the other reactions are in equilibrium. We have therefore decided to study these elementary steps in the NH_3 synthesis over a Ru catalyst using DFT calculations.

The calculated energetics for the reaction path are shown in Fig. 2. The figure shows the formation of two NH_3 molecules, both on a flat surface and on a stepped surface. First an N_2 molecule and three H_2 molecules dissociate. In the next steps the hydrogen atoms are added to the nitrogen atom one-by-one, and the most stable adsorption site and configuration are found for each number of hydrogen atoms. After addition of three H atoms, the first NH_3 molecule desorbs from the surface and the formation of the second NH_3 molecule continues. The process is exothermic by 1.8 eV for formation of two ammonia molecules. If we take zero-point energies [38,39] into account the reaction energy is -1.0 eV, which is in very good agreement with thermodynamical data (-1.0 eV) [40].

3.1. The reaction over terrace sites

To look closer at the reaction intermediates, the adsorption energies and preferred geometries found in the DFT calculations are shown in Table 1. The adsorption sites found in the calculations are in good agreement with suggested sites in the literature. The intermediates N and H both sit in a threefold hollow site [19,41–43]. Hcp sites are preferred by N, whereas H sits in an fcc site. This is in agreement with the results of Schwegmann et al. [41], who found in low-energy electron diffraction (LEED) and DFT studies that N sits in an hcp site. They determined that N is located 1.05 ± 0.05 Å above the Ru surface.

An adsorbed NH sits in an hcp site, as suggested by Staufer et al. [20]. When two hydrogen atoms have been added to the N atom our calculations suggest that the reaction intermediate moves from the hollow site to a twofold bridge site. Unfortunately we have not found experimental evidence to support this change in site, as NH_2 is unstable at room temperature (the barrier to form NH from NH_2 is very small, see Fig. 2) [18]. Rauscher et al. [16] have, however, observed NH_2 on the Ru(0001) surface at 220–280 K during hydrazine decomposition, but no suggestion of possible adsorption sites is made in their paper.

According to the calculations, the most stable adsorption site for an adsorbed NH_3 is the on-top site where the configuration is slightly tilted. In calculations where we tried to adsorb NH_3 in an hcp hollow site the molecule was not stable on the surface and desorbed. These results are in good agreement with the results from DFT studies performed by Frechard et al. of the adsorption of NH_3 on rhodium surfaces [44]. The fact that NH_3 is bound most strongly to the surface in the on-top site is not surprising. The molecule binds to the surface through the lone electron pair on the N atom. The surface bond is formed mainly from electrostatic interactions between NH_3 and the substrate. The electron-rich N atom is therefore expected to bind to the surface in the most electron-deficient site, the on-top site.

To complete the picture of the reaction path, energy barriers along the path have been calculated. The barriers found are for the hydrogenation steps (3), (4), and (5) in addition to the N_2 dissociation barrier (1). The three barriers for the addition of an H atom are similar in height. The first hydrogenation step has a barrier of about 1.2 eV/molecule and this height increases by about 0.1 eV for each hydrogen added. The heights of the calculated barriers are shown in Fig. 2 and in Table 2. Our values are in a good agreement with the results from Hu and co-workers [28]: their calculations give 1.13, 1.28, and 1.20 eV for reactions (3), (4), and (5), respectively.

As an example of the hydrogenation steps studied here, Fig. 3 shows the formation of NH_2 according to

$$\mathrm{NH}* + \mathrm{H}* \leftrightarrows \mathrm{NH_2}* + *. \tag{7}$$

In the initial state (IS) the NH adsorbate sits in an hcp site while an H atom sits in a neighboring fcc site. Next the H atom moves to the NH (TS). Finally the adsorbate complex moves to the bridge site, which is preferred by the product NH_2. The other two steps are similar to the one shown here.

3.2. The reaction at step sites

The DFT results for adsorption energies and preferred geometries for the reaction intermediate at step sites are shown in Table 3. Comparing adsorption energies for the intermediates at the step site to the energies at terrace sites (Table 1) we see that the surface species are bound stronger to the step site than the terrace site. Different surface species are stabilized by different amounts of energy, from almost no stabilization for H atoms (0.03 eV) to significant stabilization of 1.12 eV for NH_2. The reason for the stabilization

Table 1
The calculated adsorption energies and geometries for the NH_3 synthesis reaction intermediates over a flat surface

Species	Site	ΔE (eV/molecule)	h (Å)	b(N–H) (Å)	α
H	fcc	−0.52	1.08	–	–
N	hcp	−0.29	1.19	–	–
NH	hcp	−0.89	1.29	1.02	3°
NH_2	Bridge	−0.54	1.69	1.02	55°
NH_3	On-top	−1.32	2.24	1.02	55°

The first two columns show the adsorption site and the adsorption energy (ΔE) (relative to N_2(g) and H_2(g)). In the next two columns the adsorbate height over the surface (h) and the N–H bond length (b(N–H)) are shown. In the last column the angle between a surface normal and the N–H bond (α) is shown.

Table 2
The reactions studied and the calculated barriers heights, E_a, for both terrace sites and step sites

Reaction	Terraces E_a (eV/molecule)	Steps E_a (eV/molecule)
$N_2 + 2* \rightarrow 2N*$	1.9	0.4
$H_2 + 2* \rightarrow 2H*$	–	–
$N* + H* \rightarrow NH* + *$	1.2	1.1
$NH* + H* \rightarrow NH_2* + *$	1.3	1.3
$NH_2* + H* \rightarrow NH_3* + *$	1.4	1.2
$NH_3* \rightarrow NH_3 + *$	–	–

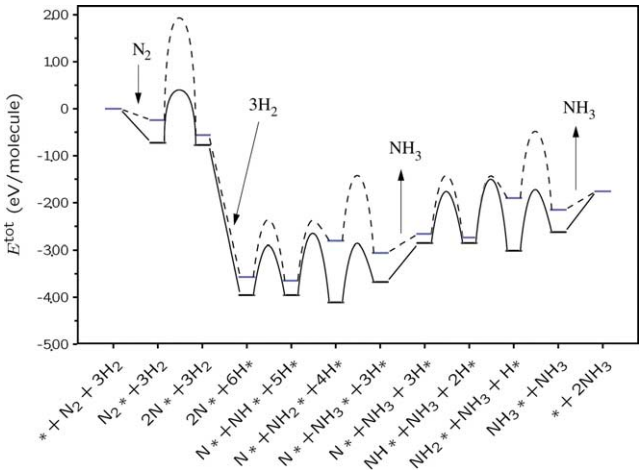

Fig. 2. Calculated energy diagram for NH_3 synthesis over a Ru surface. Both the energetics for the flat surface (dashed lines) and the stepped surface (solid lines) are shown. The formation of two ammonia molecules from N_2 and H_2 is shown.

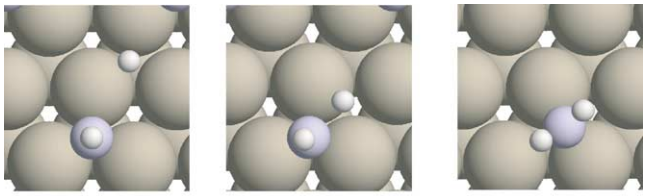

Fig. 3. The addition of a hydrogen to an adsorbed NH. First NH sits in the threefold fcc site, but during the reaction it moves over to the less coordinated bridge site. The figure shows the initial state (IS), the transition state (TS), and the final state in the reaction (FS). The energy barrier for the reaction is $E_a = 1.3$ eV/molecule estimated by DFT calculations.

is twofold. First the reactivity of Ru atoms at the step is increased due to the undercoordination of step atoms. This effect has been explained by the d-band model of Hammer and Nørskov [45]. The more step atoms the adsorbate binds to, the more pronounced this effect. The other factor is steric freedom, since at the step the adsorbate is much more free to find an energetically favorable adsorption configuration than at the terrace site.

The preferred sites for N and NH are still the hcp sites, but since they are closer to the step both intermediates are stabilized by about 0.1 eV/adsorbate. The most stable configuration for an H atom at a step site is the one where it sits at the edge of the step and is bound to two Ru step atoms.

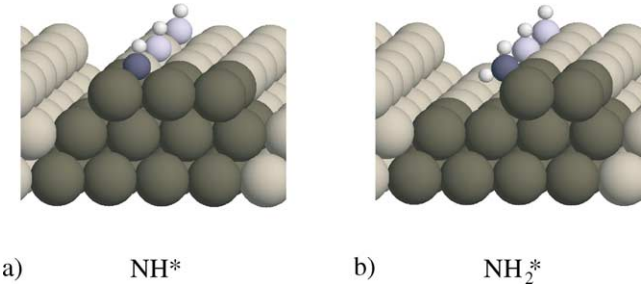

Fig. 4. The most stable configuration for (a) NH and (b) NH_2 adsorbed at a step site. The unit cell used in the calculations is indicated by the dark atoms. The size of the unit cell is (4×2) and a three-layer slab is used.

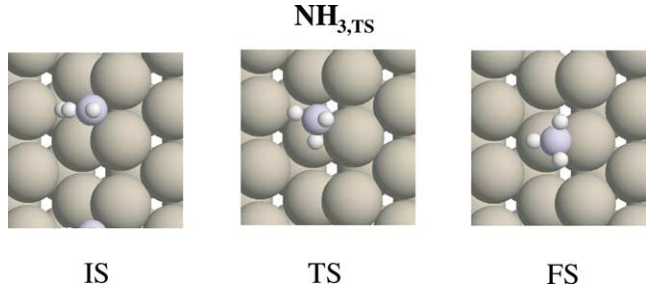

Fig. 5. The addition of a hydrogen to NH_2 adsorbed at a step site. IS denotes the initial state, TS the transition state, and FS the final state.

A similar configuration is the most stable one for the NH_2 intermediate (Fig. 4b), but where H is only stabilized by 0.03 eV NH_2 is stabilized by more than 1 eV. The cause of the large stabilization is that at the step NH_2 is able to bind at a bridge site on the step and is therefore much more free to find a stable configuration than on the terrace, even though the adsorbate is not bound to a larger number of Ru atoms at the step. NH_3 binds in a similar way as NH_2 but at an on-top site on a Ru step atom.

In addition to adsorption energies, we have calculated the barriers for the reaction at the step sites. The influence of the edge atoms is largest for N_2 dissociation, where the barrier is lowered by 1.5 eV/molecule [26]. These results are supported by experiments performed by Dahl et al. [26]. Their experiments give a N_2 dissociation barrier of (0.4 ± 0.1) eV over a Ru(0001) surface. This barrier is thus for the dissociation at the step sites and is in an excellent agreement with

Table 3
The adsorption energies and geometries for the intermediates in the NH_3 synthesis on a stepped Ru(0001) surface

Species	Site	ΔE (eV/molecule)	b(Ru–N) (Å)	b(N–H) (Å)	$\theta_{H–N–H}$	α
H	Bridge	−0.55	–	–	–	–
N	hcp	−0.40	1.99	–	–	–
NH	hcp	−0.95	2.06	1.03	–	0°
NH_2	Bridge	−1.66	2.15	1.03	113°	56°
NH_3	On-top	−1.76	2.27	1.03	109°	34°

The first two columns show the adsorption site and the adsorption energy (ΔE) (relative to N_2(g) and H_2(g)). The next two columns show the Ru–N bond length (b(Ru–N)) and the N–H bond length (b(N–H)), respectively. The two last columns show the angle $\theta_{H–N–H}$ and the angle showing how much the adsorbate is tilted relative to a surface normal (α).

our DFT calculations. The dissociation barrier for the terrace sites has been determined by Diekhöner et al. [8], where they measured the barrier through laser-assisted associative desorption. In these experiments, which are mainly sensitive to the desorption from the terraces, they estimated the dissociation barrier to be 1.8 eV, which is also in very good agreement with our DFT results.

The effect on other barriers in the reaction is not as large, the barriers for the hydrogenation steps are lowered by 0.2–0.3 eV/molecule. The reason for this is the different geometries of the transition states. In N_2 dissociation the N atoms are not only bound to the step but are also bound to a larger number of Ru atoms than in the dissociation on the terrace [26]. For the transition state configurations of the hydrogenation steps this is not the case. In these steps the transition state is bound to the same number of substrate atoms as in reaction sites on a terrace. For these reaction steps the reason for the lowering is solely the enhanced reactivity of the Ru step atoms.

Fig. 5 shows configurations along the reaction path for the addition of an H atom to NH_2. It shows the reaction path found to have the lowest barrier. In the initial state the NH_2 sits at the edge of the step and the H atom at the base of the step. This is not the most stable adsorption site for an H atom but the path gives the lowest barrier. The barrier for this reaction is 1.0 eV/molecule. As the H atom does not sit in its most favorable site, the energy difference for the two sites has to be added to the barrier. This gives a total barrier of 1.2 eV/molecule. Other reaction paths for the NH_3 formation were also investigated but they all give higher barriers.

Zhang et al. [28] have also estimated the barrier for the second hydrogenation step. Their calculations gave a barrier of 0.81 eV/molecule. This is somewhat lower than the value we find but different initial states can explain the difference. In their calculations they use as the initial state, a configuration, which is similar to configuration for NH_2 (Fig. 4b). We, on the other hand, use the one shown in Fig. 4a. This gives a difference in the calculated barrier of about 0.3 eV/molecule.

3.3. Promotion

Next, we studied the effect of promotion on the reaction paths. For the Ru catalyst electropositive alkali metals, like Cs, have been found to give the largest promotional effect [46]. In this case where the promoter atom is an electropositive alkali or alkaline earth metal atom the effect can be estimated by calculating the dipole moment (μ_{ads}) induced when the adsorbate is bound to the surface. The effect of the promoter atom has been shown to be given primarily by the electrostatic interaction between this dipole moment and the electrostatic field ε induced by the adsorbed alkali atom (ε_{alkali}) [47,48]. We therefore estimate the change in the adsorption energy due to the promotion as

$$\Delta E_{int} = -\varepsilon_{alkali}\mu_{ads}. \quad (8)$$

Table 4
The calculated dipole moment (μ_{ads}) for the transition state, $N_{2,TS}$ and the intermediates in NH_3 synthesis as a result of promotion of the surface

	Terrace μ_{ads} (eÅ)	Step μ_{ads} (eÅ)
$N_{2,TS}$	−0.13 [25]	−0.15
N	−0.03 [25]	0.01
NH	0.18	0.24
NH_2	0.25	0.27
NH_3	0.35	0.56

Table 4 shows the calculated dipole moments for configurations along the two reaction paths. According to Eq. (8) the interaction energy decreases if both μ_{ads} and ε_{alkali} are negative (the adsorbate bond becomes more stable). Mortensen et al. [25] have used DFT to estimate the electrostatic field adsorbed Na atom induces to be $\varepsilon_{Na} = -1$ V/Å.

The energy of the N_2 transition state decreases in the presence of a field of this strength and the transition state is stabilized compared to an unpromoted surface. On the other hand, other configurations studied are destabilized, except N which is almost unaffected by the presence of the promoter. The same effect is seen both for the terrace sites and the step sites but the influence is larger at the step site.

The DFT calculations therefore indicate that alkali atoms promote the NH_3 synthesis both by lowering the N_2 dissociation barrier and by lowering the coverage of other intermediates along the reaction path. This is in accordance with studies investigating the effect of electropositive promoter atoms on the reaction steps, where the increased stability of the $N_{2,TS}$ has been suggested [25,48–50] as well as the destabilization of the reaction intermediates [49,51].

3.4. The rate-limiting step

Finally, we studied which step is the rate-determining step in the reaction. Fig. 2 shows that at the step sites the N_2 dissociation step has the lowest barrier of the reaction. This raises the question whether this reaction step really is the rate-determining step of the reaction as commonly assumed [52]. To study this we have estimated the rates both for the N_2 dissociation and for the step where NH_2 is formed. The latter step is chosen because it is the step in the reaction with the highest barrier according to the DFT calculations. In the following we assume that the reaction happens at $T = 700$ K.

If we first look at the dissociation step. The rate for this step can be written as

$$r_1 = k_1 \frac{P_{N_2}}{P_o}\theta_*^2, \quad (9)$$

where

$$k_1 = A e^{-E_a/k_B T}, \quad (10)$$

P_{N_2} is the partial pressure of nitrogen, P_o is the standard pressure (1 bar), and θ_* is the number of free sites on the

surface. At the temperatures and pressure we are considering we need not include the molecularly adsorbed state explicitly, since it is in equilibrium with the gas phase and has a very low coverage. To estimate the rate constant transition state theory can be used giving

$$k_1 = \frac{k_B T}{h}\frac{q_{TS}}{q_{gas}} e^{(E_{gas}-\Delta E_{TS})/k_B T}. \quad (11)$$

Here q_{TS} and q_{gas} are the partition functions for $N_{2,TS}$ and N_2(g), respectively [53], and we define $E_{gas} = 0$. By comparing Eqs. (10) and (11) we see that the prefactor A is

$$A = \frac{k_B T}{h}\frac{q_{TS}}{q_{gas}}. \quad (12)$$

The partition function for N_2 in the gas phase can be written as

$$q_{gas} = \frac{k_B T}{2\varepsilon_{rot}}\frac{k_B T}{P_{N_2}/P_o}\left(\frac{2\pi m k_B T}{h^2}\right)^{3/2}, \quad (13)$$

when the N–N vibrations are assumed to be frozen out.[1] The rotational constant for the N_2 molecule is $\varepsilon_{rot} = 0.248$ meV [40].

To evaluate q_{TS} we have performed DFT calculations to estimate the vibrational frequencies for the N_2 in the transition state, which gives 73, 65, 58, 55, and 53 meV, respectively. These frequencies give us $q_{TS} = 10.00$ using $q_{TS} = q_{vib}$ as at the transition state both the translational and the rotational partition functions are close to unity.

Using then Eqs. (11) and (13) to estimate the prefactor we get $A = 0.241\ s^{-1}$. With these assumptions and $\Delta E_{TS} = 0.4$ eV/molecule, the rate constant for the N_2 dissociation is $k_1 = 3.2 \times 10^{-4}\ s^{-1}$.

If we now look at the rate for step (4), it can be written as

$$r_4 = k_4 \theta_{NH}\theta_H \quad (14)$$

and using Eq. (10) as

$$r_4 = A e^{-E_a/k_B T}\theta_{NH}\theta_H. \quad (15)$$

To estimate the prefactor for this step, transition-state theory can also be used. In this case the partition function for the two states can be assumed to be almost equal and close to 1. A then becomes

$$A = \frac{k_B T}{h} = 10^{13}\ s^{-1}. \quad (16)$$

For this prefactor and $E_a = 1.3$ eV, the rate constant for this step becomes $k_4 = 4400\ s^{-1}$.

These calculations show that the rate constant is lowest for the first step in the reaction. This is generally the case in the temperature range usually used in the ammonia synthesis as can be seen in Fig. 6. Furthermore, under synthesis conditions the number of free sites θ_* is low whereas θ_H and θ_{NH} are high [52], which only enhances the difference in the two rates, c.f. Eqs. (9) and (14). This shows that the N_2 dissociation is indeed the rate-determining step in the reaction under most conditions.

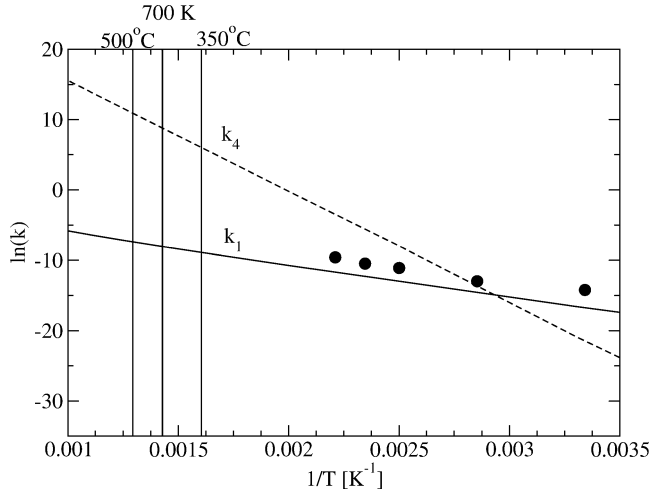

Fig. 6. The calculated rate constants k_1 and k_4 for reactions (1) and (4), respectively. The calculations show that in the temperature range used in the ammonia synthesis (350–500 °C) the rate constant for the N_2 dissociation, k_1 is lower than k_4. The insert shows the measured rate constant taken from Ref. [26] (points). The density of active sites is taken to be $1.57 \times 10^{17}\ m^{-2}$ and is found by assuming that the number of step sites is 1% of the total number of sites on the Ru(0001) surface ($1.57 \times 10^{19}\ m^{-2}$) [54].

4. Conclusion

We have presented DFT results for the elementary steps in ammonia synthesis over a Ru catalyst. The calculations show that the intermediates in the reaction are bound stronger to the active sites located at steps than on flat terraces. Based on this we suggest that the reaction mainly occurs at the step sites. We can, however, not exclude that one or more of the elementary reaction steps take place on a terrace site. It is clear from Fig. 2 that the hydrogenation of NH could take place over terrace site as well. We also conclude that the N_2 dissociation is the rate-determining step in the reaction over a Ru(0001) surface. Finally, the calculations suggest that the promotion of the reactants by alkali metals takes place by a combination of a stabilization of the transition state of the N_2 dissociation and the destabilization of NH species on the surface.

Acknowledgment

The Center for Atomic-Scale Materials Physics (CAMP) is sponsored by the Danish National Research Foundation. The DFT calculations have been performed with support from the Danish Center for Scientific Computing through grant no. HDW-1101-05.

[1] The vibrational contribution to the partition function $q_{vib} = \prod_i 1/(1 - e^{-\hbar\omega_i/k_B T})$ can be assumed to be frozen out when $\hbar\omega_i/k_B T$ is high enough. The N–N stretching mode in the gas phase has the frequency $\hbar\omega = 272$ meV [47]. At 700 K the term $\hbar\omega_i/k_B T = 4.5$ and $q_{vib} = 1.01$.

References

[1] M. Boudart, in: G. Ertl, H. Knözinger, J. Weitkamp (Eds.), Handbook of Heterogeneous Catalysis, Vol. 1, Wiley–VCH, Weinheim, 1997, p. 1.
[2] M.V. Twigg, Catalyst Handbook, Manson, London, 1996.
[3] R.B. Strait, B. Smith, H. Leonard, Ammonia Plant Safety (and Related Facilities) 38 (1998) 197.
[4] C.J.H. Jacobsen, S. Dahl, P.L. Hansen, E. Törnqvist, L. Jensen, H. Topsøe, D.V. Prip, P.B. Møenshaug, I. Chorkendorff, J. Mol. Catal. A 163 (2000) 19.
[5] H. Dietrich, P. Geng, K. Jacobi, G. Ertl, J. Chem. Phys. 104 (1995) 375.
[6] H. Shi, K. Jacobi, G. Ertl, J. Chem. Phys. 99 (1993) 9248.
[7] L. Romm, G. Katz, R. Kosloff, M. Asscher, J. Phys. Chem. 101 (1997) 2213.
[8] L. Diekhöner, H. Mortensen, A. Baurichter, A.C. Luntz, B. Hammer, Phys. Rev. Lett. 84 (2000) 4906.
[9] M.J. Murphy, J.F. Skelly, A. Hodgson, B. Hammer, J. Chem. Phys. 110 (1999) 6954.
[10] R.C. Egeberg, J.H. Larsen, I. Chorkendorff, Chem. Phys. 3 (2001) 2007.
[11] H. Dietrich, K. Jacobi, G. Ertl, J. Chem. Phys. 105 (1996) 8944.
[12] H. Dietrich, K. Jacobi, G. Ertl, Surf. Sci. 352–354 (1996) 138.
[13] J.E. Parmeter, Y. Wang, C.B. Mullins, W.H. Weinberg, J. Chem. Phys. 88 (1988) 5225.
[14] C. Benndorf, T.E. Madey, Surf. Sci. 135 (1983) 164.
[15] H. Dietrich, K. Jacobi, G. Ertl, Surf. Sci. 377–379 (1997) 308.
[16] H. Rauscher, K.L. Kostov, D. Menzell, Chem. Phys. 177 (1993) 473.
[17] J.E. Parmeter, U. Schwalke, W.H. Weinberg, J. Vacuum Sci. Technol. A 6 (1988) 847.
[18] H. Shi, K. Jacobi, G. Ertl, J. Chem. Phys. 102 (1995) 1432.
[19] K. Jacobi, H. Dietrich, G. Ertl, Appl. Surf. Sci. 121/122 (1997) 558.
[20] M. Staufer, K.M. Neyman, P. Jacob, V.A. Nasluzov, D. Menzel, N. Rösch, Surf. Sci. 369 (1996) 300.
[21] Y. Zhou, S. Akhter, J.M. White, Surf. Sci. 202 (1988) 357.
[22] J.J. Mortensen, Y. Morikawa, B. Hammer, J.K. Nørskov, J. Catal. 169 (1997) 85.
[23] D.J. Dooling, R.J. Nielsen, L.J. Broadbelt, Chem. Eng. Sci. 54 (1999) 3399.
[24] B. Hammer, Phys. Rev. B 63 (2001) 205423/1.
[25] J.J. Mortensen, B. Hammer, J.K. Nørskov, Phys. Rev. Lett. 80 (1998) 4333.
[26] S. Dahl, Á. Logadóttir, R.C. Egeberg, J.H. Larsen, I. Chorkendorff, E. Törnqvist, J.K. Nørskov, Phys. Rev. Lett. 83 (1999) 1814.
[27] T.H. Rod, Á. Logadóttir, J.K. Nørskov, J. Chem. Phys. 112 (1999) 5343.
[28] C. Zhang, Z. Liu, P. Hu, J. Chem. Phys. 115 (2001) 609.
[29] K.M. Neyman, M. Staufer, V.A. Nasluzov, N. Rösch, J. Mol. Catal. A 119 (1997) 245.
[30] W. Widdra, T. Moritz, K.L. Kostov, P. König, M. Staufer, U. Birkenheuer, Surf. Sci. 430 (1999) L558.
[31] B. Hammer, L.B. Hansen, J.K. Nørskov, Phys. Rev. B 59 (1998) 7413.
[32] D. Vanderbilt, Phys. Rev. B 41 (1990) 7892.
[33] G. Kresse, J. Furthmuller, Comput. Matter. Sci. 6 (1996) 15.
[34] H. Jónsson, G. Mills, K.W. Jacobsen, Nudged Elastic Band Method for Finding Minimum Energy Paths of Transitions, 1997.
[35] A. Ulitsky, R. Elber, J. Chem. Phys. 92 (1990) 1510.
[36] G. Ertl, in: J.R. Jennings (Ed.), Catalytic Ammonia Synthesis, Plenum, New York, 1991, p. 109.
[37] P. Stoltze, J.K. Nørskov, Phys. Rev. Lett. 55 (1985) 2502.
[38] G. Herzberg, Molecular Spectra and Molecular Structure I. Spectra of Diatomic Molecules, Krieger, Malabar, FL, 1989.
[39] G. Herzberg, Molecular Spectra and Molecular Structure II. Infrared and Raman Spectra of Polyatomic Molecules, Krieger, Malabar, FL, 1991.
[40] P.W. Atkins, Physical Chemistry, Oxford Univ. Press, Oxford, 1990.
[41] S. Schwegmann, A.P. Seitsonen, H. Dietrich, H. Bludau, H. Over, K. Jacobi, G. Ertl, Chem. Phys. Lett. 264 (1997) 680.
[42] H. Shi, K. Jacobi, Surf. Sci. 313 (1994) 289.
[43] M. Lindroos, H. Pfnür, P. Feulner, F. Menzel, Surf. Sci. 180 (1987) 237.
[44] F. Frechard, R.A. van Santen, A. Siokou, J.W. Niemantsverdriet, J. Chem. Phys. 111 (1999) 8124.
[45] B. Hammer, J.K. Nørskov, Adv. Catal. 45 (2000) 71.
[46] S. Dahl, P.A. Taylor, E. Törnqvist, I. Chorkendorff, J. Catal. 178 (1998) 679.
[47] J.J. Mortensen, L.B. Hansen, B. Hammer, J.K. Nørskov, J. Catal. 182 (1999) 479.
[48] J.K. Nørskov, S. Holloway, N.D. Lang, Surf. Sci. 137 (1984) 65.
[49] O. Hinrichsen, F. Rosowski, A. Hornung, M. Muhler, G. Ertl, J. Catal. 165 (1997) 33.
[50] G. Ertl, S.B. Lee, M. Weiss, Surf. Sci. 114 (1982) 527.
[51] D.R. Strongin, G.A. Somorjai, J. Catal. 109 (1988) 51.
[52] S. Dahl, J. Sehested, C.J.H. Jacobsen, E. Törnqvist, I. Chorkendorff, J. Catal. 192 (2000) 391.
[53] K.J. Laidler, Theories of Chemical Reaction Rates, McGraw-Hill, New York, 1969.
[54] S. Dahl, E. Törnqvist, I. Chorkendorff, J. Catal. 192 (2000) 381.